

Through space interaction between ferrocenes mediated by a thioether



G. Joel Meyer, Gabriel B. Hall, Elliott R. Smith, Takahiro Sakamoto, Dennis L. Lichtenberger*, Richard S. Glass*

Department of Chemistry and Biochemistry, The University of Arizona, Tucson, AZ 85721, USA

ARTICLE INFO

Article history:

Received 16 April 2014

Accepted 25 June 2014

Available online 2 July 2014

Keywords:

Electrostatic communication

Sulfur

Through space

Photoelectron spectroscopy

Mixed valence

ABSTRACT

A series of conformationally constrained 2,6-bisferrocenylphenyl thioethers were synthesized via Suzuki–Miyaura cross coupling reactions. Structural information was obtained using X-ray crystallography and dynamic ^1H NMR spectroscopic studies, showing highly constrained *m*-terphenyl systems. Interaction of the ferrocene moieties through space mediated by the sulfur were studied by ultra-violet photoelectron spectroscopy (UPS), cyclic voltammetry, differential pulse voltammetry, UV–Vis–NIR spectroscopy and DFT computations. Electrochemical results show two, fully reversible 1e^- redox processes for the ferrocenes where the separation of peaks is affected by both solvent and supporting electrolyte, suggesting significant electrostatic interaction which is further confirmed in the gas phase by UPS studies.

© 2014 Elsevier Ltd. All rights reserved.

1. Introduction

It is well established [1,2] that electron-rich neighboring group interactions lead to lower oxidation potentials of thioethers. This has been ascribed to lone pair–lone pair destabilization of the neutral species and 2c, 3e bonding in the 1e^- oxidized species [3,4]. It has also been suggested that sulfur–aromatic interactions may play a role in structural stabilization, protein signaling and communication in biological systems [5–8]. These interactions may have an effect on molecular recognition, redox sensing in cells, electrostatic interactions or electronic communication in proteins. The redox chemistry of thioethers may play a role in the pathogenesis of neurological disorders such as Alzheimer's and Parkinson's diseases [9–15].

Apparent stabilization of thioether radical cations by arenes has been reported based on electron paramagnetic resonance (EPR) and time-resolved fluorescence detected magnetic resonance spectroscopy [16–18]. Stacking of the cysteinyl sulfur attached to a tyrosyl radical with tryptophan and its effects on radical behavior and enzyme catalysis in galactose oxidase has been reported [19–21]. Interestingly, Morgan and coworkers suggested the possibility of electron transfer in redox proteins through S– π stacks in which sulfur side chains alternate with aromatic ones [7]. Recently, we reported evidence for S– π interaction in conformationally

constrained norbornyl compounds with juxtaposed thioether and aromatic moieties, which results in lowered oxidation potentials [22]. In these compounds, there is through space interaction resulting from mixing of the lone-pair sulfur *p*-orbital and arene π -MOs. Furthermore, it has been shown, using gamma radiolysis coupled with UV–Vis spectroscopy, that a formal S– π bond (three electron bond in the radical cation) is formed upon oxidation. However, studies on more extended interaction in *m*-terphenyl derivatives mediated by alternating S– π chains sulfur and aromatic radical cations was hampered because sulfur and aromatic radical cations are generally too reactive or unstable and decompose under cyclic voltammetry conditions resulting in irreversible oxidation of thioethers and arenes [23].

There has been much research on stable, reversibly oxidized systems in which interaction may be readily studied in their mixed valence complexes. Understanding the varying extent to which communication occurs is well documented and the spectroscopic and electrochemical techniques to observe this communication are well understood [24–31]. Due to their well-defined and relatively stable redox species, polyferrocenyl complexes are often used for the study of interactions via connecting bridges. In such studies communication is generally studied through conjugated π -frameworks; a few studies have examined the possibility of communication via a through space mechanism [27,28]. It is the goal of the present study to determine if through space interaction mediated by sulfur could be observed in a chemically stable bisferrocenyl system, and if such interactions are observed, whether the basis for such interactions were electrostatic or electronic or both.

* Corresponding authors. Tel.: +1 520 621 4472 (D.L. Lichtenberger). Tel.: +1 520 621 2939 (R.S. Glass).

E-mail addresses: dlichten@email.arizona.edu (D.L. Lichtenberger), rglass@email.arizona.edu (R.S. Glass).

2. Materials and methods

2.1. General methods and instrumentation

All reactions were carried out under inert atmosphere with standard Schlenk techniques. THF and hexane were dried and distilled prior to use according to standard methods. Thin layer chromatography (TLC) was carried out on EMD Chemical, Inc. TLC Plastic Sheets Si 60 F254. Column chromatography was performed using Dynamic Adsorbents 32–63 micron flash silica gel. 2,6-Dibromoaniline and *tert*-butyl lithium were purchased from Alfa Aesar Chemical Company. All other reagents were purchased from Aldrich Chemical Co. and were used without further purification unless otherwise stated. *tert*-Butanol was purchased from J.T. Baker Inc., 200 proof ethanol was purchased from Decon Laboratories, Inc. and all other solvents were purchased from EMD Chemical, Inc. Tetrabutylammonium tetrakis(pentafluorophenyl)borate was supplied by Boulder Scientific Co. Proton and carbon-13 nuclear magnetic resonance (NMR) spectra were recorded on Varian-300, Bruker DRX-500 and Bruker DRX-600 spectrometers. Chemical shifts are reported in parts per million using residual NMR solvent as reference. Infrared spectra were recorded on a Nicolet Impact-410 spectrophotometer. All melting points are uncorrected and were recorded on Thomas Hoover Uni-Melt apparatus. All mass spectra were done at the University of Arizona Mass Spectrometry Facility using a JEOL HX110A high resolution mass spectrometer.

2.2. Synthesis

2.2.1. 1,3-Diferrocenyl benzene (1)

This known compound was synthesized using a modification of the procedure reported by Patoux et al. [32]. 1,3-Diferrocenylbenzene was prepared from the Suzuki–Miyaura cross coupling reaction of 5 eq. of ferrocenylboronic acid in 1,4-dioxane and 3 M NaOH in the presence of a Pd(PPh₃)₂Cl₂ catalyst to afford the desired product as a red solid.

2.2.2. 2,6-Dibromobenzenethiol

A solution of NaNO₂ (205 mg, 2.97 mmol) in H₂O (1.5 mL) was added dropwise to a suspension of 2,6-dibromoaniline (678 mg, 2.70 mmol) in 12 M aqueous HCl (2.6 mL) at 0 °C. The mixture was stirred at 0 °C for 90 min. Additional NaNO₂ (55 mg, 0.80 mmol) was added. The mixture was stirred for an additional 45 min at 0 °C and then the resulting cold solution was added dropwise to a stirred solution of potassium ethylxanthate (525 mg, 3.27 mmol) in H₂O (0.65 mL) at 45 °C through a glass pipet with a plug of glass wool. The reaction mixture was stirred for 30 min at this temperature and then allowed to cool to room temperature. The reaction mixture was extracted with diethyl ether (3 × 50 mL). The combined organic extracts were washed successively with 1 M NaOH solution (100 mL), water (3 × 50 mL), brine (50 mL), dried over anhyd MgSO₄, filtered and evaporated under reduced pressure. The resulting crude product was dissolved in ethanol (8 mL) and heated to reflux. Potassium hydroxide pellets (654 mg, 11.6 mmol) were added and refluxing continued overnight. After cooling to room temperature, the ethanol was evaporated under reduced pressure. The residue was dissolved in water and washed with diethyl ether (100 mL). The aqueous layer was acidified with 1 M HCl to pH 2 and extracted with diethyl ether (3 × 50 mL). The organic extracts were washed with water (50 mL), brine (50 mL), dried over anhyd MgSO₄, filtered and evaporated under reduced pressure. The residue was purified by silica gel chromatography using hexanes as eluent to give the product as a slightly yellow solid (518 mg, 72%): ¹H

NMR (500 MHz, CD₂Cl₂) δ 5.04 (s, 1H), 6.87 (t, *J* = 7.0 Hz, 1H), 7.52 (d, *J* = 7.0 Hz, 2H); IR (KBr) 1400, 1421, 1543, 2553 (SH), 3064, 3458 cm⁻¹.

2.2.3. 2,6-Dibromo-1-(*tert*-butylthio)benzene

This compound was prepared using modified procedures [33,34]. A solution of 2,6-dibromothiophenol (180 mg, 0.671 mmol), *t*-butanol (0.332 mL, 3.49 mmol), AcOH (2.7 mL), and acetic anhydride (0.387 mL) was stirred at 0 °C for 20 min under argon, and then 70% aqueous HClO₄ (0.108 mL) was added. The solution was allowed to warm to room temperature and stirred overnight. After *t*-butanol was removed under reduced pressure, water (50 mL) was added to the solution. The solution was extracted with CH₂Cl₂ (3 × 50 mL). The combined organic layer was washed with NaOH (50 mL), brine (50 mL), dried with anhydrous MgSO₄, filtered and evaporated under reduced pressure. The resulting crude product was purified by silica gel chromatography using hexanes as eluent to give 2,6-dibromo-1-(*tert*-butylthio)benzene as a slightly yellow oil (87%-quantitative yield): ¹H NMR (600 MHz, CD₂Cl₂) δ 1.41 (s, 9H), 7.02 (t, *J* = 9.0 Hz, 1H), 7.68 (d, *J* = 9.0 Hz, 2H); ¹³C NMR (600 MHz, CD₂Cl₂) δ 32.22, 52.71, 131.64, 133.44, 135.50, 136.38; IR (neat) 1413, 1542, 2959 cm⁻¹; HRMS (GCT MS EI+, *m/z*): Calcd for C₁₀H₁₂Br₂S, 321.9026; Found: 321.9013.

2.2.4. 2,6-Diferrocenyltoluene (2)

To a solution of 2,6-dibromotoluene (15 mg, 0.06 mmol) in distilled 1,4-dioxane (0.08 mL) under argon, were added a 3 M aqueous solution of NaOH (0.11 mL), ferroceneboronic acid (90 mg, 0.4 mmol), and Pd(PPh₃)₄ (13 mg, 0.011 mmol). The reaction was stirred for 16 h. H₂O (15 mL) was added to the resulting suspension and extracted with dichloromethane (10 mL). The organic layer was washed successively with 1 M NaOH (10 mL), brine (10 mL), and H₂O (10 mL), dried with anhydrous MgSO₄, filtered and evaporated under reduced pressure. The crude product was purified by flash silica gel chromatography using 15% dichloromethane in hexanes as eluent to give 2,6-bisferrocenyltoluene as a red–orange solid (78%, *R*_f = 0.25): m.p. 139.5–141.0 °C (decomposition at 205 °C); ¹H NMR (500 MHz, CDCl₃) δ 2.27 (3 H, s), 4.22 (10 H, s), 4.26 (4H, *J* = 1.8 Hz, t), 4.42 (4H, *J* = 1.9 Hz, t), 7.21 (1H, *J* = 7.7 Hz, t), 7.73 (2H, *J* = 7.6 Hz, d); ¹³C NMR δ 13.14, 67.54, 69.49, 70.59, 89.03, 124.59, 124.59, 129.50, 134.63, 137.98; IR: 1413, 1542, 2857, 2959 cm⁻¹; HRMS (*m/z*): Calcd for C₂₇H₂₄Fe₂, 460.0576; Found: 460.05687.

2.2.5. 2,6-Bisferrocenyl-1-(*tert*-butylthio)benzene (3)

To a solution of 2,6-dibromo(*tert*-butylthio)benzene (50 mg, 0.21 mmol) in distilled 1,2-dimethoxyethane (0.2 mL) under argon, were added a 3 M aqueous solution of NaOH (0.25 mL), ferroceneboronic acid (230 mg, 1.05 mmol), and Pd(PPh₃)₄ (17 mg, 0.021 mmol). The mixture was stirred at reflux for 24 h. H₂O (15 mL) was added to the resulting suspension and extracted with dichloromethane (2 × 15 mL). The organic layer was washed successively with water (15 mL) and brine (30 mL), dried with anhyd MgSO₄, filtered and evaporated under reduced pressure. The crude product was purified by flash silica gel chromatography using 15% CH₂Cl₂ in hexanes as eluent to give 2,6-bisferrocenyl-1-(*tert*-butylthio)benzene as a red–orange solid (62% yield, *R*_f = 0.15). The product was further purified by recrystallization twice using hexanes: m.p. 184.3–185.2 °C (decomposition at 240 °C); ¹H NMR (500 MHz, CDCl₃) δ 0.65 (9 H, s), 4.18 (10 H, s), 4.26 (2H, br s), 4.30 (2H, br s), 4.40 (2H, br s), 5.00 (2H, br s), 7.34 (1H, *J* = 7.7 Hz, t), 7.83 (2H, *J* = 7.6 Hz, d); ¹³C NMR δ 30.86, 49.26, 67.15, 67.48, 69.58, 72.27, 73.24, 89.11, 127.44, 129.79, 131.08, 146.36; IR: 1413, 1535, 2857, 2960 cm⁻¹; HRMS (GCT MS EI+, *m/z*): Calcd for C₃₀H₃₀SFe₂, 534.0767; Found: 534.07623.

2.2.6. 2,6-Bisferrocenyl-1-(methylthio)benzene (**4**)

To a solution of 2,6-dibromo(methylthio)benzene (100 mg, 0.35 mmol) in distilled 1,4-dioxane (0.25 mL) under argon, were added a 3 M aqueous solution of NaOH (0.5 mL), ferroceneboronic acid (190 mg, 0.75 mmol), and Pd(PPh₃)₄ (30 mg, 0.03 mmol). The reaction was stirred for 16 h. H₂O (15 mL) was added to the resulting suspension and extracted with dichloromethane (30 mL). The organic layer was washed successively with 1 M NaOH (30 mL), brine (30 mL), and H₂O (30 mL), dried with anhyd MgSO₄, filtered and evaporated under reduced pressure. The crude product was purified by flash silica gel chromatography using 20% CH₂Cl₂ in hexanes as eluent to give 2,6-bisferrocenyl(methylthio)benzene as a red–orange solid (71% yield, *R*_f = 0.3). The product was further purified by recrystallization twice using hexanes: m.p. 198.0–198.9 °C; ¹H NMR (500 MHz, CDCl₃) δ 1.68 (3 H, s), 4.22 (10 H, s), 4.35 (4H, *J* = 1.9 Hz, t), 4.68 (4H, *J* = 1.9 Hz, t), 7.29 (1H, *J* = 7.7 Hz, t), 7.78 (2H, *J* = 7.7 Hz, d); ¹³C NMR δ 19.24, 67.67, 69.61, 71.32, 88.60, 126.14, 130.31, 135.42, 142.01. IR 1413, 1542, 2959, 3125 cm⁻¹. HRMS (*m/z*): Calcd for C₂₇H₂₄SFe₂, 492.0297; Found: 492.0306.

2.3. Crystal structure studies

The intensity data for compounds **2** and **3** were collected on a Bruker Apex II Duo CCD diffractometer, using graphite-monochromated Mo K α radiation (λ = 0.71073 Å) [35]. Crystallographic data as well as structure solution and refinement details are summarized in Table 1. The structures were solved by direct methods (SHELXS) [36] and refined by full-matrix least squares techniques against *F*² using SHELXL implemented into Olex2 [37]. All non-hydrogen atoms were refined anisotropically. All hydrogen atoms were included at calculated positions with a bond length set at 0.95 Å for aromatic H atoms, 0.99 Å for alkyl H atoms, and 0.98 Å for methyl hydrogen atoms. Thermal parameters for hydrogens were fixed as isotropic equivalents of the atom to which they were attached; 1.50 for methyl hydrogen atoms, and 1.20 for all other hydrogen atoms. Olex2 was used for structure representations [37].

2.4. Electrochemical measurements

All electrochemical experiments were carried out with a Gamry Reference 3000 potentiostat. The source and treatment of solvent and supporting electrolyte have been reported above in 2.1 General methods and instrumentation section. Voltammetric experiments were conducted at 298 K, by using approximately 1.0 mM of each compound in MeCN or CH₂Cl₂ containing 0.10 M or 0.20 M electrolyte, respectively. Bu₄NPF₆ or Bu₄NB(C₆F₅)₄ electrolytes were used, and a Glassy Carbon working Electrode (GCE) was used for all experiments, under an Ar atmosphere. All potentials are reported vs. the ferrocenium/ferrocene (Fc⁺/Fc) couple measured externally subsequent to each experiment under the same experimental conditions.

2.5. Photoelectron spectroscopy

Photoelectron spectra were recorded using an instrument that features a 360 mm radius hemispherical analyzer (McPherson) [38], with a custom-designed photon source, sample cells, detection, and control electronics. Calibration and data analysis were described previously [39]. All samples sublimed cleanly, with no visible changes in the spectra during data collection after initial observation of ionizations from the diiron compounds. The sublimation temperatures (at 10⁻⁶ Torr) were 126–136, 191–218, 108–150 and 103–194 °C for compounds **1**, **2**, **3**, and **4** respectively.

2.6. Density functional theory (DFT) computations

DFT computations were carried out with the Amsterdam density functional (ADF2013.01) package [40]. Geometry optimizations and frequency computations (with no imaginary frequencies in the final geometries) were performed in the gas phase using the VWN functional with Stoll correction implemented [41]. All electronic energies were obtained with the OPBE functional [42]. Comparison of the OPBE functional to other common functionals found it to be the best for the prediction of nuclear magnetic constants [43] and the only functional to correctly

Table 1
Crystallographic data for compounds **2** and **3**.

Parameter	3	2
Empirical formula	C ₃₀ H ₃₀ Fe ₂ S	C ₂₇ H ₂₄ Fe ₂
Formula weight	534.3	460.16
<i>T</i> (K)	100(2)	100(2)
Crystal system	triclinic	triclinic
Space group	<i>P</i> $\bar{1}$	<i>P</i> $\bar{1}$
<i>a</i> (Å)	7.3875(2)	5.8639(7)
<i>b</i> (Å)	12.8598(4)	12.8660(15)
<i>c</i> (Å)	14.4839(5)	13.2732(16)
α (°)	115.4500(10)	94.288(4)
β (°)	92.2440(10)	97.694(3)
γ (°)	105.0020(10)	101.825(4)
<i>V</i> (Å ³)	1182.15(6)	965.9(2)
<i>Z</i>	2	2
ρ_{calc} (mg/mm ³)	1.501	1.582
<i>m</i> (mm ⁻¹)	1.332	1.513
<i>F</i> (000)	556	476
Crystal size (mm)	0.080 × 0.250 × 0.300	0.239 × 0.185 × 0.105
Radiation	MoK α (λ = 0.71073)	MoK α (λ = 0.71073)
2 θ range for data collection	3.16–58.02°	3.114–56.622°
Index ranges	–6 ≤ <i>h</i> ≤ 10, –17 ≤ <i>k</i> ≤ 16, –18 ≤ <i>l</i> ≤ 19	–7 ≤ <i>h</i> ≤ 7, –16 ≤ <i>k</i> ≤ 16, –17 ≤ <i>l</i> ≤ 17
Reflections collected	20432	11220
Independent reflections (<i>R</i> _{int} , <i>R</i> _{sigma})	5529 (0.0317, 0.0321)	4431 (0.0252, 0.0324)
Data/restraints/parameters	5529/0/301	4431/0/263
Goodness-of-fit (GOF) on <i>F</i> ²	1.021	1.032
Final <i>R</i> indexes [<i>I</i> ≥ 2 σ (<i>I</i>)]	<i>R</i> ₁ = 0.0268, <i>wR</i> ₂ = 0.0643	<i>R</i> ₁ = 0.0264, <i>wR</i> ₂ = 0.0626
Final <i>R</i> indexes (all data)	<i>R</i> ₁ = 0.0355, <i>wR</i> ₂ = 0.0685	<i>R</i> ₁ = 0.0338, <i>wR</i> ₂ = 0.0666
Largest difference in peak/hole (e Å ⁻³)	0.52/–0.31	0.41/–0.33

predict the spin states of seven different iron compounds [42]. All computations utilized a triple- ζ Slater type orbital (STO) basis set with one polarization function (TZP) for H, C, Fe and S. Relativistic effects by the zero-order regular approximation (ZORA) [44,45] were also applied during all computations. The frozen-core approximation was used for the inner core of all heavy atoms. Figures of the optimized geometries and molecular orbital plots were created with the program Molekel [46].

3. Results and discussion

3.1. Synthesis of model compounds 1–4

The synthesis of the direct precursors to complexes 2–4 shown in Scheme 1 were performed by modification of published procedures [32–34]. The Suzuki–Miyaura cross coupling between ferroceneboronic acid and dibromo aryl substrates were carried out with 5 equiv of boronic acid and 1 equiv of the respective dibromide under palladium-catalyzed (10%) conditions at reflux for 16–24 h. After evaporation, the crude brown mixture was separated by column chromatography on silica gel with hexanes/ CH_2Cl_2 (85:15) to afford the pure compounds which were then, further purified by recrystallization in hexanes/ CHCl_3 and the yields are listed in Table 2.

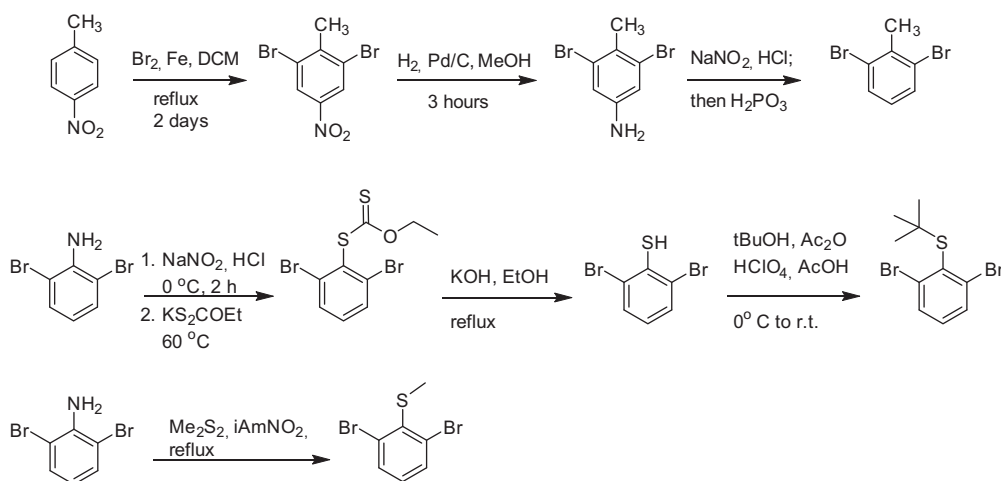
3.2. X-ray crystallography studies

The structures in the solid state for compounds 2 and 3 were determined by single crystal X-ray spectroscopic analysis. An ORTEP drawing of 2 is shown in Fig. 1 and that for 3 in Fig. 2. It is immediately noticeable that the two ferrocene rings in 2 adopt an *anti* conformation but those in 3 are *syn*. The *anti* conformation in 3 is sterically disfavored by interaction between the *syn* ferrocene ring and adjacent bulky *t*-butyl group. The structure of 1,3-diferrocenylbenzene, 1 [47], and its 5-chloro and 5-cyano derivatives [32] were also reported and, notably, the Cp rings attached to benzene in these compounds are nearly coplanar with the benzene ring (ca. 10–15° torsion angles) and the ferrocene rings adopt a *syn* conformation in one case [47] and an *anti* conformation in the others [32] suggesting that there is little difference in energy between the conformers and packing factors determine the conformation in the solid state. However, in 2 there is rotation about the Cp to benzene bonds to increase this dihedral angle (ca. 43–50°) owing to steric interaction between the interspersed methyl group and ferrocene moieties. In addition, there is a

widening of the pertinent bond angles (C7C6C1 and C17C2C1, 123.0° and 123.46° respectively) to relieve steric strain and concomitant reduction in the C17C6C5 and C7C2C3 bond angles to 117.2° and 116.8° respectively. Similarly, in 3 the Cp rings attached to the benzene ring are rotated by ca. 42–59° and the C7C6C1 and C17C2C1 bond angles increased (122.6° and 123.4° respectively) and C17C6C5 and C7C2C3 decreased (117.9° and 116.96° respectively). It is striking that the distortions caused by the methyl group and *t*-BuS group are similar. This suggests a comparable predominantly steric effect of the methyl group and sulfur atom which have comparable van der Waals radii of 2.0 and 1.85 Å, respectively [48]. However, this inference is complicated by the greater C–S than C–C bond length which results in greater cyclohexane A-values for Me versus SMe [49]. The slightly greater rotations about the Cp to benzene bonds in 3 over that in 2 despite the smaller van der Waals radius for S than methyl may be due an electronic effect of S or steric effect by the *t*-butyl group. The rotations about the Cp to benzene bonds in 2 and 3 decrease electronic interaction between the ferrocene groups and benzene ring but allow the possibility of through space interaction between the ferrocene moieties via the methyl group of 2 and the sulfur in 3.

3.3. ^1H NMR spectroscopic studies of 3 and 4

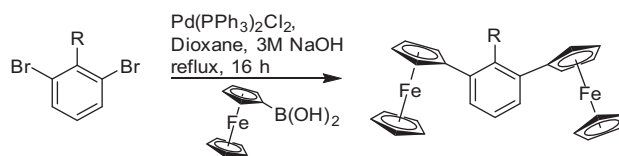
To determine if the structures of 3 and 4 in solution are the same as those determined in the solid state their ^1H NMR spectra were measured. At room temperature in CDCl_3 , 3 shows four separate proton multiplets (see Supporting information), representing an ABMX-type system on Cp rings attached to benzene as expected due to the steric interaction of the *tert*-butyl group and the geometry found in the solid state. However, the ^1H NMR spectrum of 4 shows two triplets for the Cp rings attached to benzene. This suggests that there is conformational mobility in 4 but not in 3. To determine the barrier for conformational interconversion in 3, variable temperature ^1H NMR spectroscopic data were collected. The results for 3 are shown in Fig. 3. Coalescence is observed in DMSO-d_6 at 103 °C. According to the Eyring equation, this gives an approximate energy barrier of $\Delta G^\ddagger = 86$ kJ/mol [50] which, in analogy with *m*-terphenylthioethers, [51] is assumed to be due to rotation about the Fc–Ph bond. In contrast, lowering the temperature for 4 did not result in any changes in the accessible temperature range (see Supporting information). This demonstrates a dramatic difference in barriers to rotation about the Cp to benzene bonds in 3 versus 4 consistent with the far greater steric effect encountered in such rotation with a *t*-BuS versus MeS group.



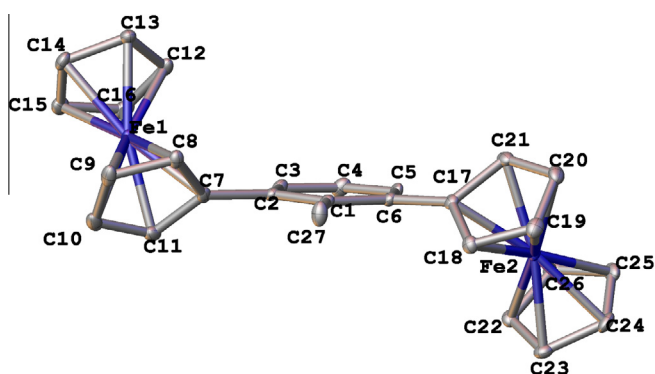
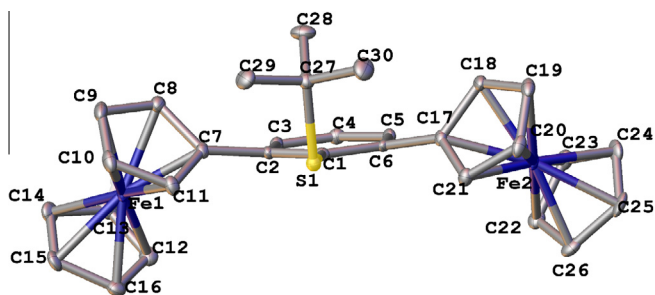
Scheme 1. Synthesis of precursor compounds to 2–4.

Table 2

Yields in the synthesis of compounds 1–4.



Compound number	R	% yield
1	H	65
2	Me	78
3	StBu	62
4	SMe	71

**Fig. 1.** ORTEP drawing of **2** showing the geometry of the Fc–Ph bonds, allowing through space interactions.**Fig. 2.** ORTEP drawing of **3** showing the almost perpendicular geometry of the Fc–Ph bonds, as well as sulfur arrangement, allowing through space interactions.

3.4. Electrochemical studies

Initial electrochemical experiments were performed in acetonitrile with *n*-Bu₄NPF₆ as supporting electrolyte. Each compound displays a reversible 2-electron oxidation as seen in Fig. 4 and the *E*_ps are listed in Table 3. Sequentially moving from compound **1** (60 mV) to **4** (23 mV), oxidation couples shift to less positive potentials which is consistent with destabilization of the HOMO due to Cp–S filled–filled interactions in compounds **3** and **4**. It was also observed that moving sequentially from **1** to **4**, redox waves broadened and a small shoulder appeared in the CV of the thioether complexes **3** and **4**, as the single 2-electron peak began to separate into two 1-electron peaks.

To reduce the stabilizing dipole interactions due to CH₃CN solvation, the experiments were repeated in CH₂Cl₂ which resulted in an increased prominence of the shoulder which was further enhanced by using differential pulse voltammetry (DPV). It was observed that two redox processes were present for the thioether

compounds **3** and **4**. However, the one 2-electron redox process for the compounds **1** and **2** remained unresolved by CV in CH₂Cl₂ with *n*-Bu₄NPF₆ as supporting electrolyte (see Supporting information) and poor resolution was observed by DPV under these conditions. However, by using *n*-Bu₄NB(C₆F₅)₄ as supporting electrolyte in CH₂Cl₂, separation into two 1e[−] reversible redox reactions was observed as seen in Fig. 5. It was previously reported [40] that cyclic voltammetry of **1** in nitrobenzene shows one pair of symmetrical redox peaks but thin layer electrochemical studies shows two separated one-electron oxidations. The separation was ascribed to communication between ferrocene centers due to electronic or perhaps electrostatic interaction. It is of interest that changing the solvent and supporting electrolyte enables separation of the two redox processes in our studies. The use of *n*-Bu₄NB(C₆F₅)₄ has been described before [52,53] and its effect ascribed to decreased ion pairing due to increased molecular diameter of the electrolyte anion, when compared with traditional electrolytes such as *n*-Bu₄NPF₆. Increased electrostatic effects in the absence of significant electronic interaction by the use electrolytes such as *n*-Bu₄N(C₆F₅)₄ has also been reported [54–56]. To determine the nature of the interaction between ferrocene centers in **2–4** spectroscopic studies on the mixed valence species were performed.

3.5. UV–Vis NIR spectroscopic investigations

Possibilities of through space interactions were further studied by spectroscopically monitoring the chemical NOBF₄ oxidation of **2–4** from FeI/FeII = FeII/FeIII = FeIII/FeIII through changes in the UV–Vis and near IR spectra. Typical ferrocenyl-type MLCT bands and d–d* transitions were observed in the ranges of 400–800 nm. In ferrocenyl-type mixed valence systems where electronic communication is observed, intervalence charge transfer transitions typically have the characteristics of a broad NIR band between 1000 and 2200 nm [57–60] that is not present in the neutral (FeI/FeII) system, increases as the species is oxidized to the mixed valence (FeII/FeIII) complex, then disappears upon further oxidation to the FeIII/FeIII system. However, no intervalence charge transfer (IVCT) bands were observed in any of the complexes.

3.6. Photoelectron spectroscopy

Gas-phase ultraviolet photoelectron spectroscopy (UPS) offers a direct experimental probe of the valence electron energies in the absence of solvent and supporting electrolyte interactions as well as providing insight into the nature (electronic as well as electrostatic) of ferrocene–ferrocene interactions [61]. The He I photoelectron spectra of **1–4** and ferrocene are shown in Fig. 6. The spectra can be segregated into three major regions and

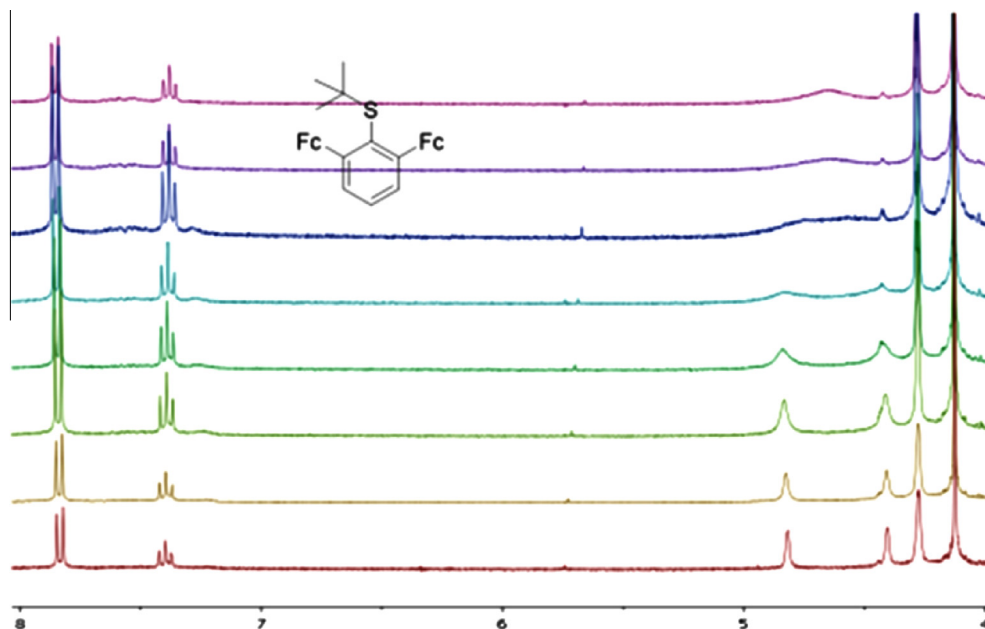


Fig. 3. Dynamic ^1H NMR spectroscopic study of **3** in DMSO from (bottom to top) 22, 35, 50, 65, 80, 95, 102, and 110 $^\circ\text{C}$. Coalescence of the Fc protons is observed at 103 $^\circ\text{C}$.

Table 3
Electrochemical data for compounds **1–4**.

	CV, MeCN, Bu_4NPF_6	CV, CH_2Cl_2 , $\text{Bu}_4\text{NB}(\text{C}_6\text{F}_5)_4$		DPV, CH_2Cl_2 , $\text{Bu}_4\text{NB}(\text{C}_6\text{F}_5)_4$
	E_p (mV)	E_1 (mV)	E_2 (mV)	ΔE_p (mV)
1	60	50	152	–100
2	34	40	156	–118
3	27	40	177	–135
4	23	53	183	–130

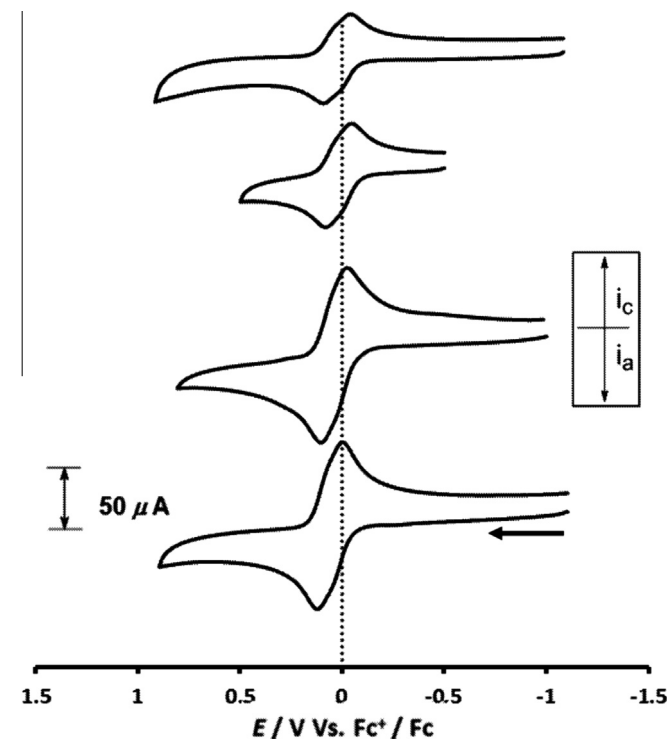


Fig. 4. Cyclic voltammograms of complexes **1–4** (bottom to top) were run in CH_3CN with 0.1 M $n\text{-Bu}_4\text{NPF}_6$ as supporting electrolyte and a glassy carbon electrode under an Ar atmosphere, with ca. 1 mM complex, and referenced to ferrocene as an external standard.

generally assigned based on ferrocene and other previously reported similar complexes [62–64]. The first region ranges from 6.2 to 7.4 eV with ionizations from primarily Fe 3d-orbitals. The second band ranges from 7.4 to 8.2 eV with ionizations from bridging ring based π -orbitals as well as primarily S based p-orbitals. The third band ranges from 8.2 to 10.1 eV with ionizations from mixed orbitals having primarily Cp ligand and some Fe character. Support of this assignment is gained from comparison of the He I

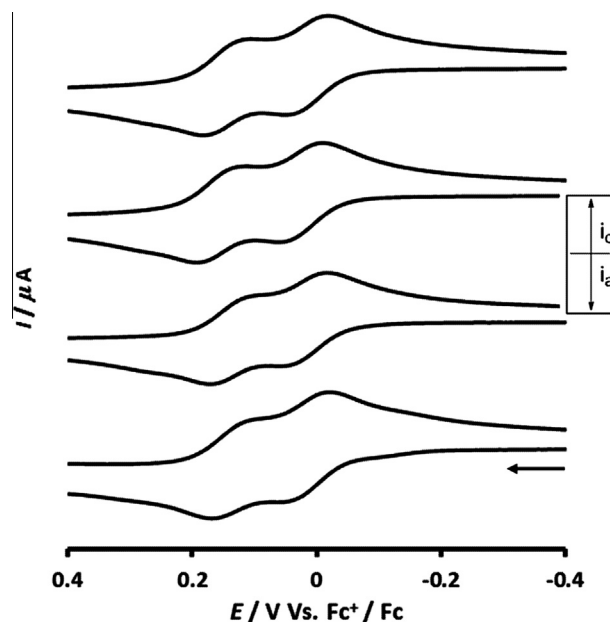


Fig. 5. Cyclic voltammograms of complexes **1–4** (bottom to top) in CH_2Cl_2 with 0.2 M, $n\text{-Bu}_4\text{NB}(\text{C}_6\text{F}_5)_4$ electrolyte and a glassy carbon electrode under an Ar atmosphere with ca. 1 mM complex, and referenced to ferrocene as an external standard.

and He II UPS shown in Fig. 7. The first range is comprised of the classic ferrocene ionizations from e_{2g} and a_{1g} ionizations [62–64].

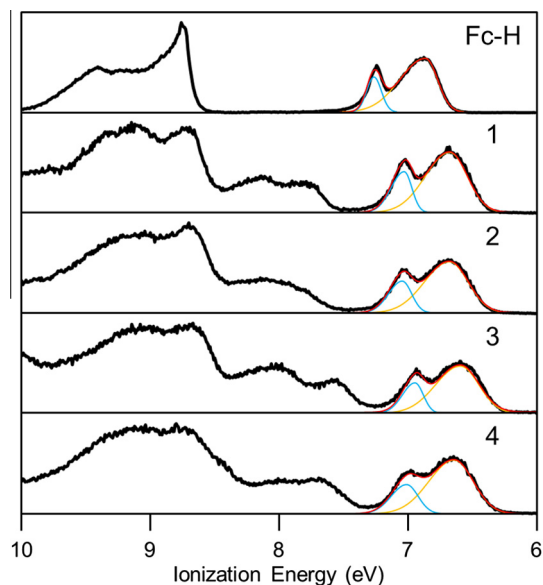


Fig. 6. He I photoelectron spectra of ferrocene (Fc-H), **1**–**4**.

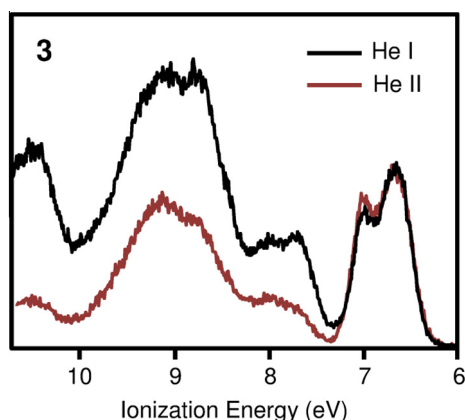


Fig. 7. Photoelectron spectra of **3**. He I (black) and He II (red). (Color online).

The second band shows a sharp decrease in relative intensity on going from He I to He II as expected for ionization from primarily S based p-orbitals as well as bridging ring based π -orbitals. A modest decrease of He II ionization intensity in the third band range suggests ionizations from primarily Cp orbitals with some Fe character.

The key to ascertaining whether there is electronic interaction between ferrocene moieties is the broadening of the lowest ionization energy band relative to ferrocene. Thus in diferrocene and bis-(μ -fulvalenediyl)diiron this band is substantially broadened relative to the comparable ferrocene band [61]. However, as seen in Fig. 6 the broadening of the lowest ionization band for **2**–**4** compared with ferrocene is modest and more consistent with vibrational broadening than electronic interaction. In all three cases the ionization energies move to lower ionization energy than that for ferrocene suggesting electrostatic interaction of the electron rich ferrocene rings. Thus the previous suggestion of electrostatic interaction between the ferrocene rings in **2** causing the splitting of the electrochemical oxidation waves is supported [40]. Interestingly, the ionizations in the first band for **4** appears to be broader than that for **3** despite the expectation of more vibrational broadening in **3** than **4**. However, this is consistent with the NMR spectroscopic studies showing greater conformational mobility in **4** than **3**.

3.7. DFT computations

The DFT computations agree with the assignments given above and also give greater insight into the nature of each ionization band. The Kohn–Sham orbitals and energies of **1**–**4** are provided in Supporting information. For all molecules the HOMO to HOMO-3 orbitals represent the e_{2g} sets of orbitals of the two ferrocenes and the HOMO-4 and HOMO-5 orbitals represent the a_{1g} orbitals of the two ferrocenes. These six orbitals are encompassed in the first ionization band from 6.2 to 7.4 eV. For **1** and **2** the HOMO-6 and HOMO-7 orbitals are primarily the highest occupied benzene pi orbitals, and these are followed by the Cp π orbitals. For **3** and **4** the S 3p based orbital is inserted as HOMO-6 and accounts for the significant decrease in He II intensity at the start of the second band at 7.4 eV. The tail end of the second band also has a significant decrease in He II intensity and is represented by the HOMO-8 orbital in which the benzene π orbital has gained some mixing with the S 3p. Ionizations from the e_{2g} and a_{1g} orbital combinations of **1** and **2** show no signs of broadening from those of ferrocene. This is in contrast to the study of bis-(μ -fulvalenediyl)diiron where significant broadening was observed in the e_{2g} ionizations due to electronic communication between the iron centers [60]. Molecule **3** may have barely perceptible broadening while **4** shows slight broadening evidenced by a diminished “valley” between the e_{2g} and a_{1g} based ionizations. The observed broadening may be due to some communication between the two metal centers, but may also be due to vibrational broadening or multiple conformations for each complex in the gas-phase. Molecule **4** has additional broadening because the optimum structure tilts the SMe group more toward one ferrocene group and renders the ferrocenes chemically inequivalent (Fig. S8). Thus the electronic communication between the two metal centers, if present, is too small to be observed. The third ionization region from 8.2 to 10.1 eV demonstrates a mild decrease in He II intensity compared to He I indicating ionizations from molecular orbitals which have primarily Cp and some iron character. The HOMO-9 to HOMO-10 represent the third ionization band and agree with the predicted character from the He I/He II analysis. The good agreement between the He I/He II analysis and the computational orbital character suggests the computations are able to model the geometric and electronic structures.

4. Conclusions

A new series of conformationally constrained bisferrocenyl phenylthioethers have been synthesized and structurally characterized to test the possibility of through space interaction mediated by the π -Cp rings and sulfur. This possibility was investigated by cyclic voltammetry, differential pulse voltammetry, DFT computations, and gas-phase photoelectron spectroscopy. Significant electrostatic interactions are observed in all systems studied and electrochemistry showed that these were greatest in **3** and **4** presumably owing to the polarizability of sulfur. No intervalence charge transfer band was observed spectroscopically in the mixed valence complexes and no evidence for electronic interaction was obtained by analysis of the UPS of **2**–**4**. The lack of electronic interaction in **3** and **4** may be due the geometry of these systems (e.g. distance) and further studies are underway to evaluate this possibility.

Acknowledgments

The authors gratefully acknowledge financial support for this work by the U. S. National Science Foundation (Grant 0956581). We would also thank Boulder Scientific Company for the generous

donation of tetrabutylammonium bromide and lithium tetrakis(pentafluorophenyl)borate.

Appendix A. Supplementary data

CCDC 996647 and 996648 contains the supplementary crystallographic data for **2** and **4**. These data can be obtained free of charge via <http://www.ccdc.cam.ac.uk/conts/retrieving.html>, or from the Cambridge Crystallographic Data Centre, 12 Union Road, Cambridge CB2 1EZ, UK; fax: (+44) 1223-336-033; or e-mail: deposit@ccdc.cam.ac.uk. Supplementary data associated with this article can be found, in the online version, at <http://dx.doi.org/10.1016/j.poly.2014.06.050>.

References

- [1] R.S. Glass, in: C. Chatgililoglu, K.-D. Asmus (Eds.), *Sulfur-Centered Reactive Intermediates in Chemistry and Biology*, NATO ASI series 197, Plenum Press, New York, 1990, p. 213.
- [2] R.S. Glass, *Rev. Heteroatom. Chem.* 15 (1996) 1.
- [3] R.S. Glass, in: S. Oae (Ed.), *Reviews on Heteroatom Chemistry*, vol. 15, MYU, Tokyo, 1996, p. 1.
- [4] C.H. Hendon, D.R. Carbery, A. Walsh, *Chem. Sci.* 5 (2014) 1390.
- [5] R.S. Morgan, D.E. Tatsch, R.H. Gushard, J.M. McAdon, P.K. Warme, *Int. J. Pept. Protein Res.* 11 (1978) 209.
- [6] R.J. Zauhar, C.L. Colbert, R.S. Morgan, W.J. Walsh, *Biopolymers* 53 (2000) 233.
- [7] J.M. Thornton, K. Reid, *FEBS* 190 (1985) 2951.
- [8] B. Geise, M. Grabber, M. Cordes, *Curr. Opin. Chem. Biol.* 12 (2008) 755.
- [9] D.A. Butterfield, *Free Radical Res.* 36 (2002) 1307.
- [10] D.A. Butterfield, *Curr. Med. Chem.* 10 (2003) 2651.
- [11] C. Schöneich, *Biochim. Biophys. Acta* 1703 (2005) 111.
- [12] S. Varadarajan, S. Yatin, J. Kanski, F. Jahanashahi, D.A. Butterfield, *Brain Res. Bull.* 50 (1999) 133.
- [13] D. Pogocki, *Chem. Res. Toxicol.* 17 (2004) 325.
- [14] D. Boyd-Kimball, H.M. Abdul, T. Reed, R. Sultana, D.A. Butterfield, *Chem. Res. Toxicol.* 17 (2004) 1743.
- [15] D.A. Butterfield, J. Kanski, *Peptides* 23 (2002) 129.
- [16] D.W. Werst, A.D. Trifunac, *J. Phys. Chem.* 95 (1991) 3466.
- [17] D.W. Werst, *J. Am. Chem. Soc.* 113 (1991) 4345.
- [18] D.W. Werst, *J. Phys. Chem.* 96 (1992) 3640.
- [19] N. Ito, S.E.V. Phillips, C. Stevens, Z.B. Ogel, M.J. McPherson, J.N. Keen, K.D.S. Yadav, P.F. Knowles, *Nature* 350 (1991) 87.
- [20] T. Ito, S.E.V. Phillips, K.D.S.W. Yadav, P.F. Knowles, *J. Mol. Biol.* 238 (1994) 74.
- [21] M.S. Rogers, E.M. Tyler, N. Akyumani, C.R. Curtis, R.K. Spooner, S.E. Deacon, S. Tamber, S.J. Firbank, K. Mahmoud, P.F. Knowles, S.E.V. Phillips, M.J. McPherson, D.M. Dooley, *Biochemistry* 46 (2007) 4606.
- [22] N.P.-A. Monney, T. Bally, G.S. Bhagavathy, R.S. Glass, *Org. Lett.* 15 (2013) 4932.
- [23] T. Yamamoto, N.P.-A. Monney, M. Ammam, P. Filipiak, S.A. Roberts, E.R. Smith, G.S. Wilson, G. Hug, C. Schoeneich, T. Bally, R.S. Glass, in preparation.
- [24] S. Barlow, D. O'Hare, *Chem. Rev.* 97 (1997) 637.
- [25] K.D. Demadis, C.M. Hartshorn, T.J. Meyer, *Chem. Rev.* 101 (2001) 2655.
- [26] F.M. D'Alessandro, F.R. Keene, *Chem. Soc. Rev.* 35 (2006) 424.
- [27] O. Wenger, *J. Hankache, Chem. Rev.* 111 (2011) 5138.
- [28] A. Heckmann, C. Lambert, *Angew. Chem., Int. Ed.* 51 (2012) 326.
- [29] B.S. Brunshwig, C. Creutz, N. Sutin, *Chem. Soc. Rev.* 31 (2002) 168.
- [30] J. Casado, S.R. González, M.C. Ruiz Delgado, M. Moreno Oliva, J.T. López Navarrete, R. Caballero, P. de la Cruz, F. Langa, *Chem. Eur. J.* 151 (2009) 2548.
- [31] S.R. González, M.C. RuizDelgado, R. Caballero, P. De la Cruz, F. Langa, J.T. López Navarrete, J. Casado, *J. Am. Chem. Soc.* 134 (2012) 5675.
- [32] C. Patoux, C. Coudret, J.-P. Launay, C. Joachim, A. Gourdon, *Inorg. Chem.* 36 (1997) 5037.
- [33] M. Dieguez, A. Ruiz, C. Claver, F. Doro, M.G. Sanna, S. Gladioli, *Inorg. Chim. Acta* 357 (2004) 2957.
- [34] T. Yamamoto, *Synthesis of Models for Neighboring Proline Amide and Aryl Participation in Electron Transfer from Thioethers*, Ph.D. Dissertation, The University of Arizona, 2011.
- [35] Bruker, APEX2, SAINT and SADABS, Bruker AXS Inc., Madison, Wisconsin, USA, 2009.
- [36] G.M. Sheldrick, *Acta Crystallogr., Sect. A* 64 (2008) 112.
- [37] O.V. Dolomanov, L.J. Bourhis, R.J. Gildea, J.A.K. Howard, H. Puschmann, *J. Appl. Crystallogr.* 42 (2009) 339.
- [38] K. Siegbahn, C. Nordling, A. Fahlman, R. Nordberg, in *ESCA: Atomic, Molecular and Solid State Structure Studied by Means of Electron Spectroscopy*; Uppsala, Almqvist & Wiksells, 1967.
- [39] M.A. Cranswick, A. Dawson, J.J.A. Cooney, N.E. Gruhn, D.L. Lichtenberger, J.H. Enemark, *Inorg. Chem.* 46 (2007) 10639.
- [40] (a) G. Te Velde, F.M. Bickelhaupt, E.J. Baerends, C. Fonseca Guerra, S.J.A. Van Gisbergen, J.G. Snijders, T. Ziegler, *J. Comput. Chem.* 22 (2001) 931; (b) ADF2013.01, 2013.
- [41] H. Stoll, C.M.E. Pavlidou, H. Preuss, *Theor. Chim. Acta* 49 (1978) 143.
- [42] M. Swart, A.W. Ehlers, K. Lammertsma, *Mol. Phys.* 102 (2004) 2467.
- [43] Y. Zhang, H. Lin, D.G. Truhlar, *J. Chem. Theory Comput.* 3 (2007) 378.
- [44] E. van Lenthe, E.J. Baerends, J.G. Snijders, *J. Chem. Phys.* 99 (1993) 4597.
- [45] E. van Lenthe, A. Ehlers, E. Baerends, *J. Chem. Phys.* 110 (1999) 8943.
- [46] S. Portmann, H.P. Luthi, *Chimia* 54 (2000) 766.
- [47] M.C.P. Wang, Y. Li, N. Merouh, H.-Z. Yu, *Electrochim. Acta* 53 (2008) 7720.
- [48] L. Pauling, *The Nature of the Chemical Bond*, third ed., Cornell University Press, Ithaca, NY, 1960.
- [49] C.H. Bushweller, in: E. Juaristi (Ed.), *Conformational Behavior of Six-membered Rings. Analysis, Dynamics and Stereoelectronic Effects*, Wiley-VCH, NY, 1995, p. 25.
- [50] H. Günther, *NMR Spectroscopy: Basic Principles, Concepts and Examples for Organic Chemistry and Structural Biology*, second ed., Wiley, New York, 1992, p. 343.
- [51] U.I. Zakai, A. Bloch-Mechkour, N.E. Jacobsen, L. Abrell, G. Lin, G.S. Nichol, T. Bally, R.S. Glass, *J. Org. Chem.* 75 (2010) 8363.
- [52] R.J. LeSuer, C. Buttolph, W.E. Geiger, *Anal. Chem.* 76 (2004) 6395.
- [53] A. Fry, in: P.T. Kissinger, W.R. Heineman (Eds.), *Laboratory Techniques in Electroanalytical Chemistry*, second ed., Marcel Dekker, New York, 1996 (Chapter 15).
- [54] F. Barrière, W.E. Geiger, *J. Am. Chem. Soc.* 128 (2006) 3980.
- [55] A.K. Diallo, J.-C. Daran, F. Varret, J. Ruiz, D. Astruc, *Angew. Chem., Int. Ed.* 48 (2009) 3141.
- [56] A.K. Diallo, C. Absalon, J. Ruiz, D. Astruc, *J. Am. Chem. Soc.* 133 (2011) 629.
- [57] N.S. Hush, *Progr. Inorg. Chem.* 8 (1967) 391.
- [58] N.S. Hush, *Coord. Chem. Rev.* 64 (1985) 135.
- [59] J.D. Launay, *Chem. Soc. Rev.* 30 (2001) 386.
- [60] P. Day, N.S. Hush, R.J. Clark, *Philos. Trans. R. Soc. A* 366 (2008) 5.
- [61] D.L. Lichtenberger, H. Fan, N.E. Gruhn, *J. Organomet. Chem.* 666 (2003) 75.
- [62] C. Cauletti, J.C. Green, M.R. Kelly, P. Powell, J. Van Tilborg, J. Robbins, J. Smart, *J. Electron Spectrosc. Relat. Phenom.* 19 (1980) 327.
- [63] S. Evans, M.L.J. Green, B. Jewitt, A.F. Orchard, C.F. Pygall, *J. Chem. Soc., Faraday Trans. 2* (68) (1847) 1972.
- [64] R. Gleiter, M.C. Boehm, R.D. Ernst, *J. Electron Spectrosc. Relat. Phenom.* 33 (1984) 269.